Virology 392 (2009) 238–245

Contents lists available at ScienceDirect

Virology

journal homepage: www.elsevier.com/locate/yviro

A tymovirus with an atypical 3′-UTR illuminates the possibilities for 3′-UTR evolution

Ioannis E. Tzanetakis [a,1], Ching-Hsiu Tsai [b], Robert R. Martin [c], Theo W. Dreher [a,d,*]

[a] Department of Microbiology, Oregon State University, Corvallis, OR 97331, USA
[b] Graduate Institute of Biotechnology, National Chung Hsing University, Taichung, Taiwan
[c] USDA-ARS, Horticultural Crops Research Laboratory, Corvallis, OR 97330, USA
[d] Center for Genome Research and Biocomputing, Oregon State University, Corvallis, OR 97331, USA

ARTICLE INFO

Article history:
Received 20 May 2009
Returned to author for revision 19 June 2009
Accepted 24 June 2009
Available online 6 August 2009

Keywords:
Tymoviridae
Recombination
Chimera
3′-UTR structure
3′-UTR evolution

ABSTRACT

We report the complete genome sequence of *Dulcamara mottle virus* (DuMV), confirming its membership within the *Tymovirus* genus, which was previously based on physical and pathology evidence. The 5′-untranslated region (UTR) and coding region of DuMV RNA have the typical characteristics of tymoviral RNAs. In contrast, the 3′-UTR is the longest and most unusual yet reported for a tymovirus, possessing an internal poly(A) tract, lacking a 3′-tRNA-like structure (TLS) and terminating at the 3′-end with –UUC instead of the typical –CC(A). An expressible cDNA clone was constructed and shown to be capable of producing infectious DuMV genomic RNAs with –UUC 3′-termini. A chimeric *Turnip yellow mosaic virus* (TYMV) genome bearing the DuMV 3′-UTR in place of the normal TLS was constructed in order to investigate the ability of the TYMV replication proteins to amplify RNAs with –UUC instead of –CC(A) 3′-termini. The chimeric genome was shown to be capable of replication and systemic spread in plants, although amplification was very limited. These experiments suggest the way in which DuMV may have evolved from a typical tymovirus, and illuminate the ways in which viral 3′-UTRs in general can evolve.

Introduction

The 3′-untranslated regions (UTRs) of positive strand RNA viral genomes harbor important cis-acting signals directing translation and replication. These are acted upon by host and viral factors that support and regulate these processes (Dreher, 1999), which may simultaneously involve elements in both the 5′ and 3′-UTR (Filomatori et al., 2006; Guo et al., 2001; Hu et al., 2007; Wu et al., 2009). These considerations suggest the existence (to varying extents for different viruses) of interdependencies between the 5′ and 3′-UTR on the one hand, and viral proteins and 3′-UTR on the other hand, that constrain 3′-UTR evolution. We have employed tymoviruses, with their very distinctive 3′-tRNA-like structure (TLS), to explore the constraints and possibilities for 3′-UTR evolution.

Turnip yellow mosaic virus (TYMV), the prototypical tymovirus, is a positive strand RNA virus with a 6.3 kb genome bearing a 5′ ^{m7}GpppG cap and a 3′-TLS that remarkably mimics the structural and functional properties of tRNA^{Val} (Dreher, 2009; Dreher and Goodwin, 1998; Dreher et al., 1992). The TYMV TLS serves a critical function that depends on its tRNA mimicry, as evidenced by the loss of viral amplification and infectivity in response to mutations that prevent its aminoacylation (Tsai and Dreher, 1991). The known tRNA-like functions of the TLS are to serve as a translational enhancer through a synergistic interaction with the 5′-cap (Matsuda et al., 2004; Matsuda and Dreher, 2004) and to maintain an intact –CCA 3′-end (Dreher and Goodwin, 1998). Viral infectivity puts little demand for sequence specificity on the TLS, since conversion of the TLS identity from valine to methionine (Dreher et al., 1996) or replacement with other valine-specific tymoviral TLSs that carry many sequence differences (Skuzeski et al., 1996) does not obliterate infectivity.

These engineered genomes were all capable of aminoacylation, but it has even been possible to produce infectious chimeric TYMV genomes with non-aminoacylatable 3′-ends based on a mutated *Tobacco mosaic virus* (TMV) TLS or the *Erysimum latent virus* (ErLV) tymoviral 3′-UTR (Goodwin et al., 1997). These experiments have cumulatively shown that there are ready opportunities for TYMV 3′-UTR evolution, even though the native 3′-UTR contains a highly specialized and functionally important element. The TLS can thus be considered as a modular element that may be replaced as a step in evolution with an appropriate heterologous segment. Such recombinations to generate chimeric genomes have indeed occurred naturally in the evolution of the tymoviruses, the majority of whose genomes possess a TYMV-like TLS. *Nemesia ring necrosis virus* (NeRNV) is a tymovirus with a typical tobamoviral histidine-specific TLS (Koenig et al., 2005a), whereas ErLV has a 3′-UTR that may be considered to include a vestigial TLS (Dreher and Goodwin, 1998).

The above considerations show that, in the case of TYMV and probably tymoviruses in general, the 3′-UTR can be considered as a

* Corresponding author. Department of Microbiology, 220 Nash Hall, Oregon State University, Corvallis, OR, 97331, USA. Fax: +1 541 737 0496.
E-mail address: theo.dreher@oregonstate.edu (T.W. Dreher).
[1] Present address: Department of Plant Pathology, Division of Agriculture, University of Arkansas, Fayetteville, AR 772701, USA.

0042-6822/$ – see front matter © 2009 Elsevier Inc. All rights reserved.
doi:10.1016/j.virol.2009.06.041

modular element that largely provides self-contained functions. For TYMV, there are evidently few constraints in terms of co-evolution between 5′ and 3′ genome termini and between the viral proteins and sequence elements in the 3′-UTR. Our understanding of the molecular features controlling translation and replication are compatible with this conclusion. First, TYMV RNA translation is synergistically enhanced by the 5′-cap and 3′-UTR, but we have observed no co-dependency in translational protein expression between 5′ sequences and the 3′-UTR (Matsuda et al., 2004; Matsuda and Dreher, 2004; Matsuda and Dreher, 2007). Second, cell-free minus strand synthesis studies with TYMV replicase preparations have shown that the sole sequence feature in the 3′-UTR that is necessary for minus strand synthesis is the 3′-terminal –CC(A) (Deiman et al., 1998; Singh and Dreher, 1998).

All the infectious natural and engineered tymoviral RNAs discussed above have –CC(A) 3′-termini, and the results from the cell-free replication experiments suggested that this could be a mandatory requirement for tymoviral RNAs. We were thus intrigued by a partial genome sequence from *Dulcamara mottle virus* (DuMV) RNA suggesting that the genome may terminate in a poly(A)-tail (GenBank accession No. AF035634). We report here the complete genome sequence of DuMV RNA and show that the reported poly(A) exists within the 3′-UTR but not at the end. Intriguingly, however, the 3′-end is atypical for a tymovirus in a different way, in both lacking a TLS and a 3′-terminal –CC(A), terminating instead with –UUC. We verify that DuMV RNAs with –UUC termini are indeed infectious by generating genomic RNA de novo from an infectious cDNA clone. Further, by constructing a chimeric TYMV genome with a DuMV-derived 3′-UTR, we show that the TYMV replication proteins are able to replicate to a limited degree genomic RNAs with –UUC rather than the native –CC (A) termini. Our studies show that the evolutionary constraints on the 3′-UTR of TYMV RNA are remarkably relaxed.

Results

DuMV genome characterization

The complete genome of DuMV (GenBank accession No. AY789137) consists of 6181 nucleotides (nt) with the base distribution 23% adenine, 32% cytosine, 17% guanine and 28% uracil. The skewed C and G compositions are characteristic of tymoviruses, although other tymoviral genomes have as high as 44.8% C and as low as 13.1% G. As for TYMV, both genomic and subgenomic RNAs are 5′-capped (see Materials and methods).

The coding region of the genome reveals characteristics that are typical of tymoviruses. It spans an almost unbroken tract from nucleotide 130 to nucleotide 5936 comprising three ORFs (Fig. 1A). As is typical of tymoviruses, the two ORFs that are expressed from the genomic RNA are extensively overlapping (Haenni and Dreher, 2008). The 5′-most ORF encodes a 62 kDa protein that is generically known as overlapping protein (OP). TYMV OP is necessary for viral spread (Bozarth et al., 1992) and is a suppressor of RNAi (Chen et al., 2004).

The ORF encoding the 196 kDa replication protein (RP) starts seven nucleotides downstream of the OP start codon, a feature common to all tymoviral genomes sequenced to date. The close spacing of the start codons of the OP and RP ORFs enables robust dicistronic expression via initiation coupling, as demonstrated with TYMV RNA (Matsuda and Dreher, 2006). Sequence motifs readily allow identification of the four typical enzymatic domains of RP (Fig. 1B): methyltransferase (MT) (Rozanov et al., 1992); papain-like proteinase (PRO) (Bransom and Dreher, 1994; Marchler-Bauer et al., 2007; Rozanov et al., 1995) with the catalytic Cys and His residues predicted at amino acid positions 681 and 767, respectively (Bransom and Dreher, 1994); RNA helicase (HEL) (Candresse et al., 1990); and RNA-dependent RNA polymerase (POL) (Koonin, 1991). TYMV RP is expressed as a polyprotein that is matured by two PRO-catalyzed cleavages located between PRO and HEL (Jakubiec et al., 2007), and between HEL and POL (Bransom et al., 1996; Kadaré et al., 1995). By aligning tymoviral RPs, DuMV RP is predicted to undergo proteolytic maturation cleavages at Gly_{777}/Ala_{778} and Gly_{1157}/Asp_{1158} (Jakubiec et al., 2007).

The tymobox, a 16 nucleotide sequence conserved in tymoviral RNAs preceding the start site of the subgenomic RNA (Ding et al., 1990a) was found between nucleotides 5336 and 5351. The tymobox is associated with an initiation box (CAAU) that covers the subgenomic RNA start site (Ding et al., 1990a). This sequence is present at nucleotides 5360–5363, suggesting initiation of the coat protein (CP) sgRNA at nucleotide A5361 (Fig. 1C). This was confirmed by 5′ RACE. DuMV CP has 90% sequence identity with the CP of Belladonna mottle virus (BeMV) (Ding et al., 1990b), suggesting that DuMV and BeMV could be strains of the same virus. Sequences outside the CP ORF, which would settle this question, are not available at present for BeMV. DuMV does not appear to be more closely related to any particular tymovirus on the basis of phylogenetic tree analysis of RP domains and CP, but is firmly a member of the tymovirus clade (Haenni and Dreher, 2008; Segwagwe et al., 2008; Stephan et al., 2008). CP and RP sequence identities to other tymoviruses range between 34% and 51% for CP and 48% and 54% for RP. These identity levels are similar between other tymoviruses. OP is the most variable tymoviral protein, with 23% to 32% sequence identity.

The 5′-UTR of the genome is 129 nt long and can be folded into three stem–loops with C·C or A·C mismatches (Fig. 2). Stem–loop

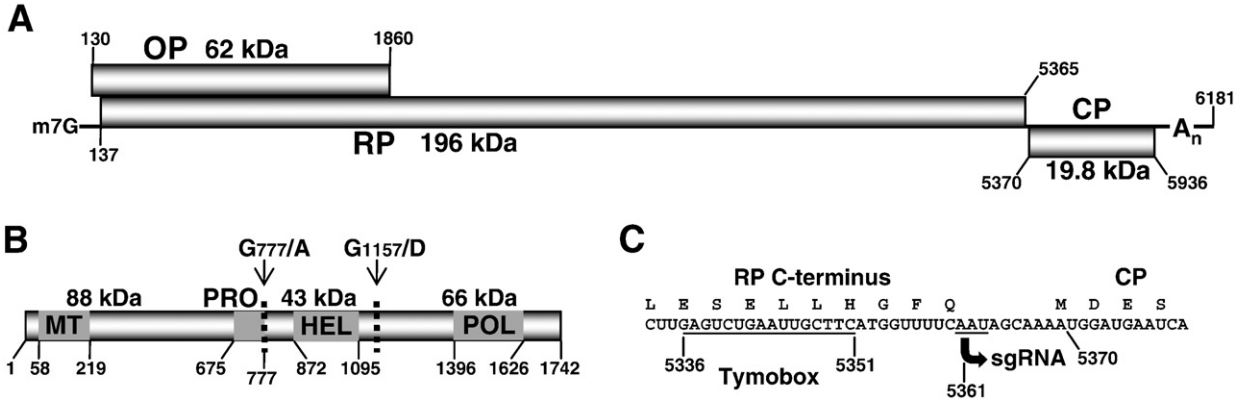

Fig. 1. (A) Representation of the genome of *Dulcamara mottle virus* with the coordinates of the first and last nucleotides of the coding regions: OP, overlapping protein; RP, replication protein; CP, coat protein. A_n represents the poly(A) tract within the 3′-UTR. (B) Representation of the RP protein, showing its enzymatic domains and predicted polyprotein cleavage sites with amino acid coordinates. MT, methyltransferase; PRO, papain-like proteinase; HEL, RNA helicase; POL, RNA-dependent RNA polymerase. (C) The sequence surrounding the tymobox (underlined), which overlaps the C-terminal region of the RP ORF, and the subgenomic RNA initiation site.

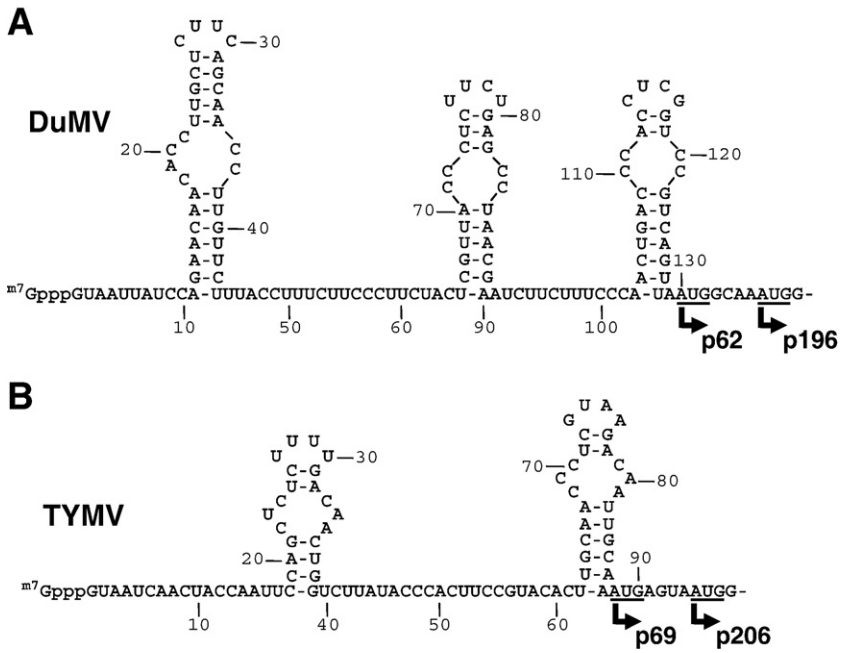

Fig. 2. Protonatable hairpins in the predicted secondary structure of the 5′-UTR of DuMV RNA (A) compared to the TYMV 5′-UTR (B), whose secondary structure has been determined experimentally (Hellendoorn et al., 1996). The start codons of the OP ORFs (p62 and p69) and RP ORFs (p196 and p206) are indicated.

structures with C·C, A·C or C·A mismatches are present in all tymovirus 5′-UTRs sequenced to date (Hellendoorn et al., 1996; Koenig et al., 2005b). At low pH, when some of these A or C residues become protonated, base-pairing occurs between the mismatches, resulting in stabilized hairpins (Hellendoorn et al., 1996). Genetic evidence supports a functional role for these protonatable hairpins during the infection (Hellendoorn et al., 1997), with a role in RNA encapsidation supported by some experiments (Bink et al., 2003; Hellendoorn et al., 1997) but not others (Shin et al., 2009). The number of protonatable hairpins in tymoviral 5′-UTRs ranges from one to four, with the downstream-most hairpin typically situated just upstream of the OP AUG initiation codon (Fig. 2).

A unique tymoviral 3′-UTR

The 245 nucleotide long DuMV 3′-UTR is the longest tymoviral 3′-UTR yet reported. The typical tymoviral 3′-UTR includes a valine-specific, approximately 82 nucleotide long TLS and up to 70 additional upstream nucleotides, although the tobamoviral-like 3′-UTR of NeRNV is 174 nucleotides long (Koenig et al., 2005a). A TLS is conspicuously lacking from the DuMV 3′-UTR, only the second such case (with ErLV; (Srifah et al., 1992) among tymoviruses. A further difference from the typical tymoviral RNA is the presence of –UUC at the 3′-terminus instead of the –CC(A) found in all other tymoviral RNAs.

An internal poly(A) tract allows division of the 3′-UTR into three sections (Fig. 3). The poly(A) tract begins 41 nucleotides downstream of the UGA CP termination codon and is 45 nucleotides long with one interspersed nucleotide (G_{6008}) in the reference sequence deposited with GenBank (accession no. NC_007609). The poly(A) length varied between cDNA clones with 6/9 being 45 nt, 1/9 48 nt and 2/9 52 nt (all length differences occurring upstream of G_{6008}). Length heterogeneity is typical for homopolymeric tracts, presumably due to polymerase slippage during replication and to some extent during the cloning process. Internal poly(A) tracts have been reported in the intergenic region of *Brome mosaic virus* RNA3 (16–22 nt in length) (Ahlquist et al., 1981) and in the 3′-UTRs of *Barley stripe mosaic virus* RNAs (BSMV; 8–40 nt long) (Kozlov et al., 1984), Hibiscus latent Singapore virus RNA (HLSV, 37–96 nt long) (Srinivasan et al., 2005) and Chikungunya alphavirus RNA (CHIK, 19–106 nt long) (Khan et al., 2002). The BSMV and HLSV poly(A) tracts are positioned immediately downstream of the stop codon, while the poly(A) tract of CHIK RNA is positioned within the 3′-UTR as with DuMV.

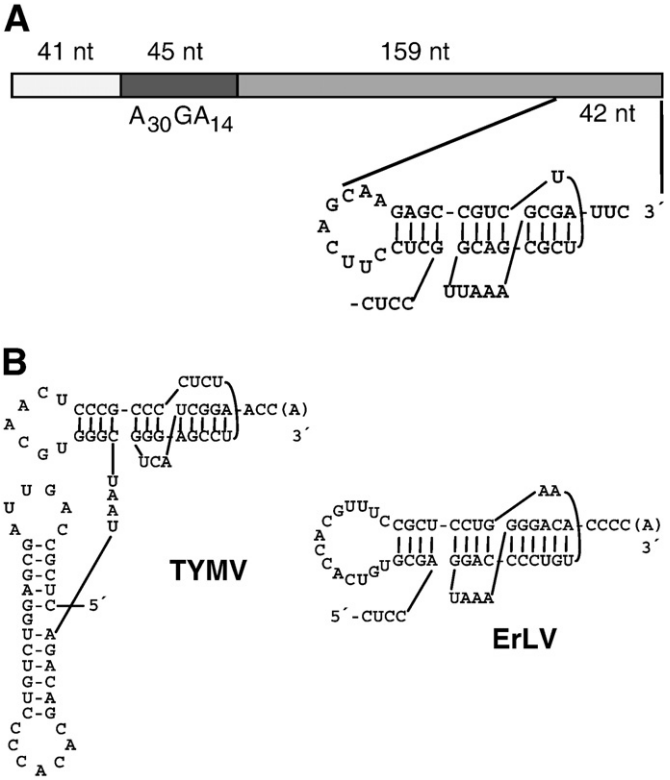

Fig. 3. (A) The 3′-UTR of DuMV RNA divided into three domains by the internal poly(A) tract. A proposed conformation for the 3′ 42 nucleotides includes a pseudoknot that allows formation of a 12 bp interrupted helix that has structural similarities to the amino acid acceptor stem (top half) of the TYMV TLS and a proposed structural feature at the 3′-end of *Erysimum latent virus* RNA (shown in B).

The 145 nt downstream of the poly(A) tract are predicted by mfold (Zuker, 2003) to contain some short hairpins and an accessible (non-base-paired) –UUC 3′-end. A pseudoknot involving the 3′-most hairpin can be predicted, and this feature can be extended to produce a structural element with 12 base-pairs (bp) that has some resemblance to the amino acid acceptor arm of tymoviral TLSs (Fig. 3). However, the 12 bp acceptor stems of the tymoviral family of TLSs are built of 4 bp/3 bp/5 bp or 3 bp/3 bp/6 bp segments (Dreher and Goodwin, 1998; Goodwin and Dreher, 1998) distinct from the 4 bp/4 bp/4 bp stem we propose for DuMV RNA (Fig. 3A). L1, the connecting string that crosses the major groove of the pseudoknot helix (Fig. 3A), which is only one nt long, is also unusually short. This should not preclude pseudoknot formation, however, since the TYMV acceptor stem pseudoknot (shown in Fig. 3B) is retained when L1 is shortened from four to one nucleotide (Mans et al., 1992).

It seems significant that a feature resembling the top half of the TYMV TLS appears to be present at the 3′-end of both non-canonical tymoviral 3′-UTRs, in DuMV and ErLV RNAs (Fig. 3). The pesudoknot-containing amino acid acceptor stem of TYMV RNA ensures the presentation of the single-stranded 3′-terminal –ACCA in an accessible non-base-paired form (Dreher, 2009). Pseudoknot-containing stems may in general act as spacers to allow optimum presentation of an accessible 3′-terminus. Since TYMV replicase requires an accessible non-base-paired –CCA initiation box for minus strand synthesis in vitro (Deiman et al., 1998; Singh and Dreher, 1998), this may be an important requirement for the viability of all tymoviral RNAs.

Both DuMV and TYMV replicases can amplify genomes with –UUC 3′-termini

The majority of TYMV virion RNAs terminate with –CC at their 3′-ends, with about 15% of RNAs terminating in –CCA. It is believed that immediately upon disencapsidation, –CC termini are converted to –CCA, with adenylation catalyzed by the host tRNA-specific enzyme CCA-nucleotidyltransferase (Dreher and Goodwin, 1998). The –CCA terminus allows full expression of the tRNA-like properties of the TLS and also serves as the primary sequence controlling minus strand initiation, as demonstrated in cell-free experiments with TYMV replicase (Deiman et al., 1998; Singh and Dreher, 1998). The presence of –CC(A) at the 3′-ends of all previously sequenced tymoviral RNAs, including the atypical RNA of ErLV (Fig. 3B) seemed to underline the importance of the 3′-terminal initiation box in controlling replication. We were thus motivated to explore the replication properties of tymoviral genomic RNAs with –UUC 3′-ends.

We constructed an infectious cDNA clone of DuMV RNA (pDuMV) by inserting the genome sequence between a T7 promoter and a BstBI restriction site. Linearization of template DNA with BstBI was expected to result in genomic transcripts terminating in –UUCg. Inoculation of *Nicotiana benthamiana* plants with 5′-capped transcripts from pDuMV/BstBI resulted in infection in 8 of 9 inoculated plants. Symptom onset was observed 9–10 days post-inoculation, two days later than for inoculation with DuMV virion RNA. Mature symptoms were similar to those produced by wild type infections (Fig. 4A). The delay in disease progression was eliminated upon inoculating new *N. benthamiana* plants with infected tissue or purified virus from these plants, and virus could then be recovered in similar yield to that of wild type infections (about 0.6 mg virus/g tissue). Viral RNA progeny isolated from systemically infected leaves and detected by Northern blotting are shown in Fig. 4. The presence of the expected –UUC 3′-termini in progeny RNAs was verified by 3′-RACE, which involved both A-tailing or C-tailing (see Materials and methods). When leaf dips of purified virus, either from infections resulting from virion RNA or infectious clone inoculation, were observed under the electron microscope more than 60% of the virions appeared empty ($n = 300$) (Fig. 4B). These results, although different from the 70–80% full particles typically observed for other tymoviruses, are similar to the observations of Gibbs et al. (1966). These experiments verify the infectivity of genomic RNA generated from pDuMV and the production of replicating RNAs with –UUC 3′-ends.

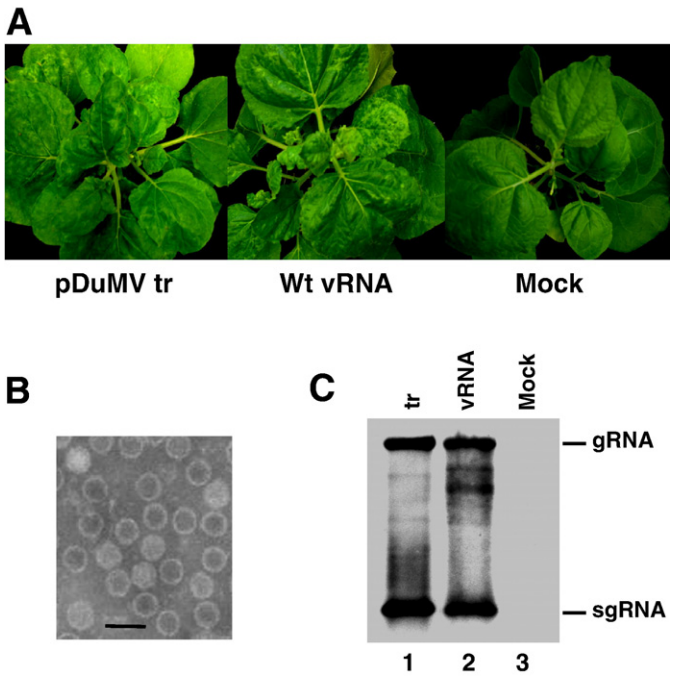

Fig. 4. Infection of *N. benthamiana* plants with RNA transcripts produced from genomic cDNA clone of DuMV RNA. A. Chlorotic mottle symptoms on plants 10 days after inoculation with 2 μg of capped transcripts made from pDuMV linearized with BstBI *Dulcamara mottle virus* (DuMV) (left) or with 1 μg of wild type DuMV virion RNA (middle panel). B. Electron micrograph of negatively stained virions isolated from plants inoculated with genomic transcripts made from pDuMV. The bar represents 50 nm. C. Detection of DuMV progeny RNAs from systemically infected leaves by Northern blotting after electrophoresis in a 1% agarose gel with chemiluminescence using a DIG-labeled probe: gRNA, genomic RNA; sgRNA, subgenomic RNA. Lane 1: analysis of 2 μg total RNA extracted from a plant inoculated with transcripts made from pDuMV; lane 2: analysis of 1 μg total RNA extracted from a plant inoculated with wild type DuMV virion RNA; lane 3: analysis of 2 μg total RNA from a healthy plant (mock).

Although DuMV is an outlier among tymoviruses in respect to the properties of the 3′-UTR, the DuMV replication protein (RP) is not a phylogenetic outlier in relation to other tymoviral RPs (Haenni and Dreher, 2008; Segwagwe et al., 2008; Stephan et al., 2008). One might therefore postulate that the unusual –UUC 3′-end evolved from the typical tymoviral –CC(A) terminus, and that this was permitted because tymoviral RPs have some, perhaps reduced, ability to use –UUC in place of –CC(A) for driving minus strand synthesis.

To test this idea, we constructed chimeric genomes with reciprocal exchanges of the entire 3′-UTRs between TYMV and DuMV RNAs (Fig. 5A). In view of the integrated function of the 3′-UTR and its TLS as deduced from studies with TYMV (Dreher, 1999), we did not produce chimeras with switches of only the 3′ initiation box sequence: TYMV infectivity depends on TLS function (Tsai and Dreher, 1991), which depends on the 3′-CCA. The chimeric genomes were inoculated to both *N. benthamiana* and Chinese cabbage plants. DuMV/3′TY chimeric RNA failed to replicate in either host (four plants of each inoculated), but the amplification of TYMV/3′Du chimeric RNA was detected in the inoculated leaf in all four Chinese cabbage plants (host for TYMV), though not in *N. benthamiana* (non-host for TYMV, but host for DuMV). Low levels of amplification were observed in the inoculated leaves by Northern blotting, with the presence of sgRNA confirming that RNA replication was occurring (Fig. 5B). The slower migration of chimeric sgRNA verifies the presence of the longer DuMV 3′-UTR in RNA that is detected with a probe that hybridizes to the

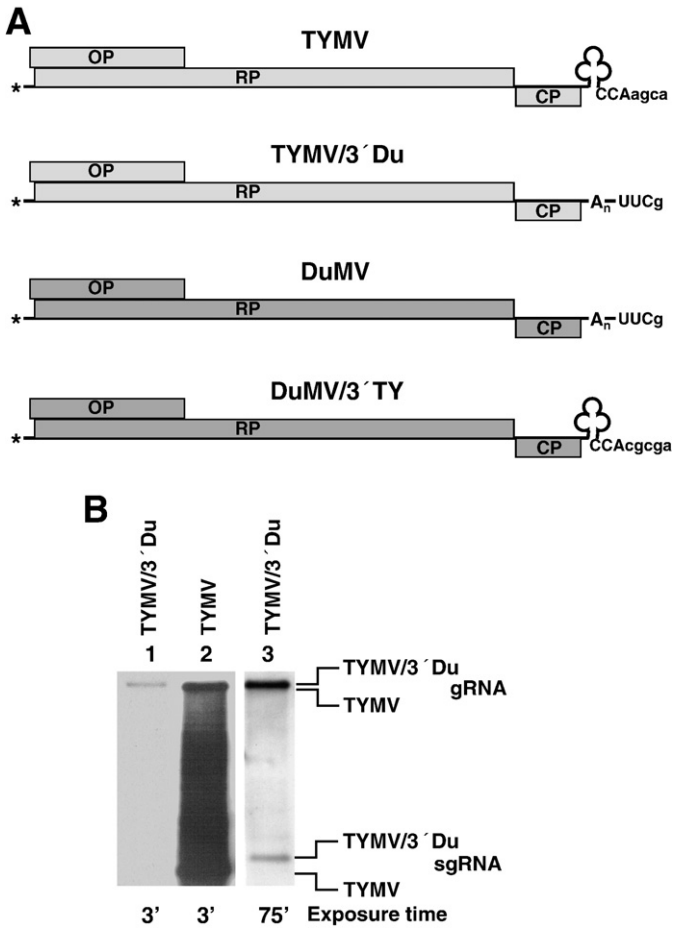

Fig. 5. Low-level replication of chimeric TYMV/3′Du RNA. (A) Diagrams of the chimeric TYMV/3′Du and DuMV/3′TY RNA genomes that contain reciprocal exchanges of 3′-UTRs. Lower case letters at the 3′-ends represent the expected non-viral nucleotides that result from run-off transcription at BstBI and MluI restriction sites. (B) Northern blot detection of progeny TYMV/3′Du RNAs in the inoculated leaves of Chinese cabbage plants at 7 dpi using a DIG-labeled probe hybridizing to the TYMV CP ORF. Note that TYMV/3′Du RNA is 142 nucleotide longer than TYMV RNA. Lanes 1 and 3: analysis of 5 μg total RNA isolated from a plant inoculated with 5 μg of TYMV/3′Du RNA transcripts (lane 1, 3 min exposure; lane 3, 75 min exposure); lane 2: analysis of 100 ng total RNA from a plant inoculated with wild type TYMV virion RNA (3 min exposure). Bent lines point to the size differences between the genomic and subgenomic RNAs of TYMV and TYMV/3′Du.

TYMV CP ORF. The levels of sgRNA were consistently lower than gRNA, whereas they are similar in the case of TYMV infections. A similarly depressed level of sgRNA was observed for some TYMV chimeric genomes with heterologous 3′-termini (Skuzeski et al., 1996).

Systemic movement of TYMV/3′Du RNA was severely impaired. TYMV/3′Du chimeric RNA was undetectable in systemic leaves by Northern blotting, and could be detected by reverse transcription PCR in only one out of the four plants tested, and then only after 40 PCR cycles. Confirmation of systemic movement of the TYMV/Du chimeras was also confirmed by sequencing of the PCR amplicons. No symptoms developed in the inoculated leaves, and plants remained asymptomatic for 6 months post-inoculation. Passaging of virus from inoculated leaves onto new plants in the hope of isolating chimeric genomes adapted to improved replication was not successful (on the basis of detection by reverse transcriptase-PCR), underlining the low efficiency of the amplification of the chimeric genome.

Discussion

DuMV was discovered in the 1960s in *Solanum dulcamara* and its host range is limited to the *Solanaceae* family. The virus can be transmitted mechanically, by *Psylloides affinis* (family *Chrysomelidae*) in a non-persistent manner, and very inefficiently by seed. These properties in addition to the virion structure, stability and serological similarities to other tymoviruses placed DuMV in the genus *Tymovirus* (Gibbs et al., 1966).

By determining the complete genome of DuMV RNA and observing typical tymoviral features in the 5′-UTR and coding regions, we are left with no doubt that DuMV is a tymovirus. The genome sequence revealed an entirely uncharacteristic 3′-UTR, however, that is the longest yet observed for a tymovirus (245 nt), possesses an internal poly(A) tract and lacks the two characteristic features of tymoviral 3′-UTRs, a TLS and a –CC(A) terminus. Although ErLV RNA was already known to possess a 3′-UTR without a TLS, it does nevertheless terminate in –CC and is an active, though poor, substrate for 3′-adenylation by the CCA-nucleotidyltransferase, indicating a residual tRNA character (Dreher and Goodwin, 1998). With a –UUC 3′-terminus, DuMV RNA lacks even the –CC(A) terminus that has to date been a property of all tymoviral RNAs. This is significant both from the point of view of loss of a feature that is characteristic of the tRNA-like features that are a hallmark of typical tymoviral RNAs and the alteration of the –CC(A) initiation box that controls minus strand synthesis (Deiman et al., 1998; Singh and Dreher, 1998).

How might DuMV have evolved as such an unusual tymovirus? As discussed in the Introduction, previous experiments with TYMV have shown that the critically important valine-specific TLS can be replaced in a modular way with certain elements from heterologous 3′-UTRs. The TYMV 3′-UTR serves as a strong translational enhancer (Matsuda and Dreher, 2004), enhances RNA stability and maintains an intact 3′-terminus (Dreher and Goodwin, 1998; Matsuda and Dreher, 2004), and provides the 3′-terminal –CCA initiation box that serves as the promoter for minus strand synthesis (Deiman et al., 1998; Singh and Dreher, 1998). Heterologous 3′-UTRs must be able to provide these functions to be part of an infectious RNA. We have observed that the 3′-UTRs of non-aminoacylatable chimeric TYMV RNAs that are derived from TMV and ErLV RNAs (Goodwin et al., 1997) do indeed provide translational enhancement (D. Matsuda and T. W. Dreher, unpublished). By terminating in –CC(A) at the 3′-end, it is also readily understandable how these RNAs could be replicated by the TYMV replication complex.

The absence of a 3′ –CC(A) to serve as a minus strand initiation box motivated our experiments with chimeric exchanges between the TYMV and DuMV 3′-UTRs. One of these, TYMV/3′Du, with TYMV 5′-UTR and coding region fused to the entire DuMV 3′-UTR, was able to replicate in Chinese cabbage and spread to systemic leaves. Replication and spread were quite inefficient, and in initial attempts we were not able to select progeny with enhanced replication due to secondary mutations. Nevertheless, the replicating RNAs did preserve their –UUC 3′-termini and did not acquire –CC(A) termini. This limited replication clearly illustrates a potential pathway for the evolution from a typical tymovirus like TYMV to DuMV. The TYMV replication complex is evidently able to replicate RNAs with –UUC 3′-termini, and some level of replication provides the opportunity for the incorporation of secondary mutations that could improve replication. The replicases of other tymoviruses with conventional –CC(A) termini might have an inherently higher ability to replicate RNAs with –UUC termini.

Our experiments thus provide a plausible pathway for the evolution of DuMV from a conventional TYMV-like tymovirus (Fig. 6). A recombinant generated by template switching to a heterologous RNA during plus strand synthesis might initially have produced a genome with a 3′-segment terminating in –UUC. NeRNV RNA, with its typical tobamoviral 3′-UTR (Koenig et al., 2005a), is clear evidence that recombination has been part of the history of the tymoviruses. Alternatively, a –UUC 3′-end might have been generated by partial loss of the 3′-UTR by RNase cleavage. Replication, initially probably at very low levels, could then have been followed by adaptive mutations that

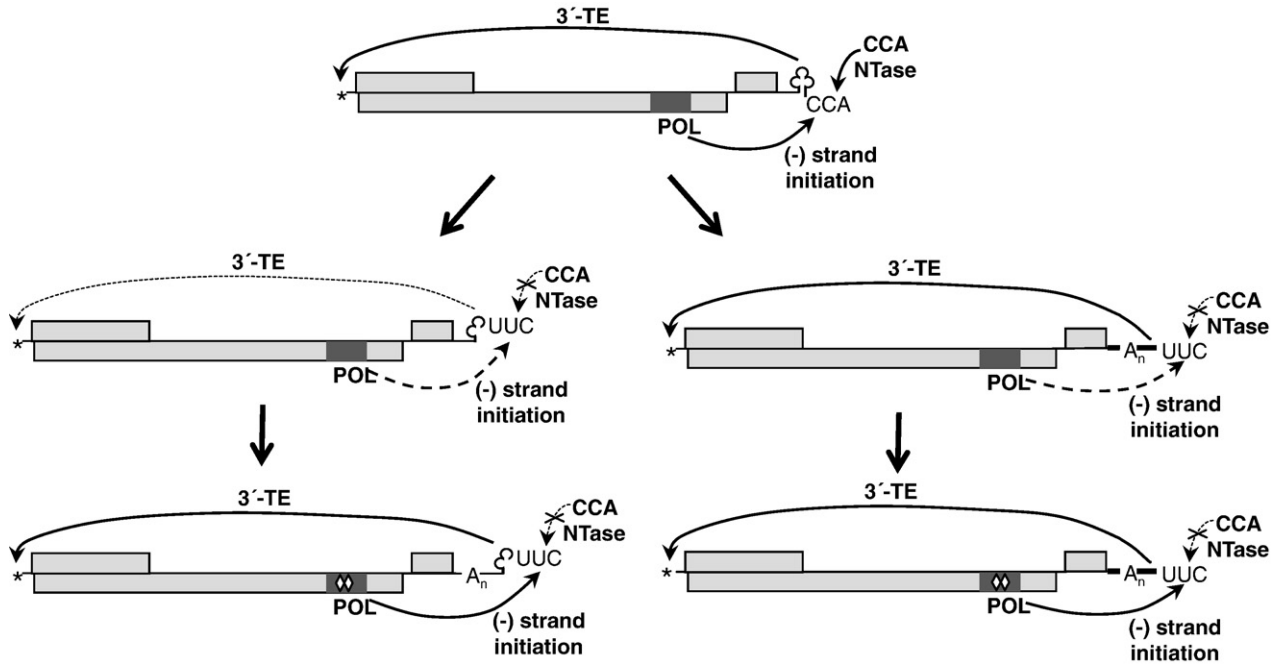

Fig. 6. Possible steps in the evolution of DuMV from a typical tymovirus, such as TYMV. The TYMV-like progenitor shown at the top has a 3′-UTR with a TLS (cloverleaf) terminating in –CCA. Three key properties of the 3′-UTR that are important for amplification and infectivity are indicated: (i) the –CCA 3′-terminus is recognized by the viral replication complex (POL) to drive minus strand initiation and replication; (ii) the 3′-UTR serves as translational enhancer (3′-TE) through synergy with the 5′-cap (*), and (iii) the 3′-terminus is maintained through the action of host CCA-nucleotidyltransferase (CCA-NTase). The classical tymovirus 3′-UTR could be lost by truncation (left arrow) to reveal an internal –UUC as the new 3′-terminus. This would decrease all 3′-UTR properties (dashed lines or X) and result in poor replication (as observed for the TYMV-3′-Du chimera). These deficiencies could then corrected by acquired mutations, such as mutations in POL (◊◊) that allow improved initiation at the –UUC 3′-terminus, and expansion of an oligo(A) tract to form an internal poly(A) (A_n) that might provide improved translational enhancement. In an alternative evolutionary sequence, shown on the right, a DuMV-like 3′-UTR could be acquired by recombination to form a hybrid much like the TYMV/3′-Du RNA we have studied. This chimeric genome would possess a 3′ translational enhancer, but adaptation of POL would be needed to acquire efficient replication and infectivity. Genomes lacking a TLS and 3′-CCA would need to rely on a strategy other than the use of CCA-NTase for stabilizing the 3′-end.

improved replication and ensured viability, including the incorporation of a pseudoknot into the 3′-terminal helix (Fig. 3).

DuMV is the only tymovirus known to contain a homopolymer stretch in the 3′-UTR. The 19–106 nt-long poly(A) tract within the 3′-UTR of CHIK S27 RNA observed by (Khan et al., 2002) appears to have arisen during multiple passages in cultured mosquito cells from A_4 or A_6 sequence patches. A similar expansion may have occurred during DuMV evolution, possibly along with other events that have produced the longest tymoviral 3′-UTR.

In summary, the description of the DuMV genome and our experiments showing the viability of chimeric TYMV/3′Du RNA have illuminated the ways in which viral 3′-UTRs can evolve to produce variants with quite different characteristics. The –UUC 3′-end of DuMV RNA is a notable deviation from the –CC/–CC(A) 3′-termini that serve as minus strand initiation sites of many non-polyadenylated viral RNA genomes (Yoshinari et al., 2000). Nevertheless, globally, viral RNA-dependent RNA polymerases seem to possess flexibility with regard to the initiation dinucleotide (van Dijk et al., 2004), and our results show that this is true to a limited degree for the TYMV enzyme. We have thus observed with the TYMV system an entire switch of the 3′-UTR including the minus strand initiation site away from tymoviral norm. Some viruses thus evidently allow considerable room for 3′-UTR evolution. This will not be true of all viruses, because in other cases known dependencies between sequences at the 5′ and 3′-ends of the genome must constrain changes in the 3′-UTR (Filomatori et al., 2006; Guo et al., 2001; Hu et al., 2007; Wu et al., 2009).

Materials and methods

Genome sequence determination and analysis

A British DuMV isolate (Gibbs et al., 1966) was amplified in *N. benthamiana* and used for determination of the genome sequence. Double-stranded RNA (dsRNA) was extracted as previously described (Yoshikawa and Converse, 1990). Virus was prepared according to Lane (1986) and viral RNA was recovered after phenol/chloroform extraction and ethanol precipitation.

cDNA synthesis and cloning followed the random hexamer priming procedure of Tzanetakis et al. (2005), using pCR 4.0 vector and Mach One (Invitrogen) *E. coli* competent cells. Clones were sequenced by Macrogen Inc. (Seoul, South Korea) on an ABI 3700 DNA sequencer. This shotgun sequencing revealed the complete genome other than about 250 nucleotides at the 5′ and 3′-ends.

The 5′-termini of both the virion genomic and subgenomic RNAs were obtained using a 5′-RACE procedure (GeneRacer, Invitrogen). This involves oligomer ligation to the 5′-terminus after treatment with alkaline phosphatase and tobacco acid pyrophosphatase (to remove the cap structure), followed by PCR amplification with priming from within the ligated oligomer. No amplification products were observed in control reactions omitting the pyrophosphatase step, indicating the presence of a 5′-cap on both genomic and subgenomic RNAs.

The sequence of the very 3′-terminus was obtained by direct RNA sequencing of genomic virion RNA with ribonucleases T1, T2 and A after 3′-end labeling with [5′-^{32}P]pCp and T4 RNA ligase as described (Dreher et al., 1989). More extensive 3′-terminal sequence was acquired after poly(A) and poly(C) tailing of dsRNA as described (Tzanetakis and Martin, 2004). The consensus sequence of the viral genome represents at least 4× coverage.

DuMV infectious cDNA clone construction

Reverse transcription PCR using genomic virion RNA as template was conducted to obtain full-length clones capable of supporting in vitro transcription of genomic RNA. Reverse transcription used 8 μg of viral RNA, primer DuMV-R (5′ GATC**GGTACC*TTCGAA***TCGCTTTAACGTCGCGAA;

KpnI site in bold and BstBI linearization site in bold italics) and 200 U Superscript II (Invitrogen). After removal of RNA with 2 U RNaseH (Invitrogen) and 5 U RNase T1 (Sigma), cDNA was purified with the QIAquick PCR Purification Kit (Qiagen). PCR was carried out with LA Taq polymerase (Takara) and the amplification primers DuMV-R and DuMV-F (5′ GATC**GGTACC***TAATACGACTCACTATA*GTAATTATCCAGAACAA; KpnI site in bold, T7 promoter in italics), used at 400 nM. The PCR program consisted of an initial cycle of 1 min at 94 °C, 30 s at 55 °C and 7.5 min at 72 °C, followed by 29 cycles of 94 °C for 30 s, 60 °C for 30 s and 72 °C for 7.5 min, with a final 20 min extension at 72 °C. The amplicon was purified from a 0.8% agarose gel using crystal violet for visualization of the DNA, and was cloned into TOPO pCR 4.0 and MegaX DH10B T1R *E. coli* cells (Invitrogen). The redundant T7 promoter in the vector was excised by removal of the NotI–SnaBI vector fragment, end-filling with the Klenow fragment of DNA polymerase I and religation using T4 DNA ligase (Fermentas). The expected DuMV-plasmid junction regions of the resultant clone pDuMV were confirmed by direct sequencing.

Construction of chimeric genomes

Two-step mutagenic PCR was employed in order to develop chimeric cDNAs with 3′-UTR switches between TYMV and DuMV: pTYMC/3′Du and pDuMV/3′TY. The TYMV/3′Du chimeric genome had a 3′-UTR that included the upstream pseudoknot region from the TYMV 3′-UTR that is thought to serve as a structural spacer element (Matsuda and Dreher, 2004); this was placed upstream of the entire DuMV 3′-UTR. To make the TYMV/3′Du chimeric fragment, two initial products with modified termini were made with primer pairs (a) TYMV-SmaIF (5′ AAATGATGAACCCCCGGGTCAAAGAT) and TYMV-DuMV 3′ fusion R (5′ AACTGGCGAGCTAACGATTTT) using pTYMC (Weiland and Dreher, 1989) as template and (b) TYMV-DuMV3′F fusion (5′ AAATCGTTAGCTCGCCAG**TTTCTTCACACTTCAGAGC**) and DuMV 3′R BstBI/HindIII (5′ TGTGCCAAGCTT*TTCGAA***GAATCGCTT-TAACGTCGC**; HindIII site underlined, BstBI site in italics, DuMV sequences in bold) using pDuMV as template. After 30 amplification cycles, the PCR products were diluted 1:10,000 and mixed, and a second PCR was conducted using primers TYMV-SmaIF and DuMV 3′R BstBI/HindIII to produce a chimeric TYMV/3′DuMV product. The final PCR product was cloned into pCR4.0 and sequenced to verify the intended sequence.

A similar approach was used to make the DuMV/3′TYMV chimeric fragment, in which the entire TYMV 3′-UTR was placed immediately downstream of the DuMV CP termination codon. The primer pairs used in this case were DuMV SmaIF (5′ **GCATATCTGCCCCCGGGTTCA**)/DuMV-TYMV3′ fusion R (5′ AACGATTTTAAAGATCGAGAAC**TTA-GAGTGCCTGCAAGAGAG**) and DuMV-TYMV3′F fusion (5′ **CTCTCTTGCAGGCACTCTAA**GTTCTCGATCTTTAAAAT)/TYMV3′R MluI/KpnI (5′ TATATCGTACG*ACGCGT*GGTTCCGATGACCCTCGG; BsiWI site underlined, MluI site in italics, DuMV sequences in bold). The SmaI/HindIII TYMV/3′DuMV and SmaI/BsiWI DuMV/3′TYMV fragments were used to replace the 3′-terminal regions of pTYMC and pDuMV to make the chimeric genomic clones pTYMC/3′Du and pDuMV/3′TY, respectively.

In vitro transcription and plant inoculation

Plasmids pDuMV and pTYMC/3′Du were linearized with BstBI, whereas pDuMV/3′TY was linearized with MluI. Plasmid DNA (1 μg) was transcribed using a T7 RNA polymerase transcription kit to make 5′ ^{m7}GpppG-capped RNA (mMessage mMachine T7; Ambion). Transcripts were ethanol precipitated and used for mechanical inoculation: 2 μg of DuMV genomic transcripts, 1 μg of DuMV wild type virion RNA (used as control) or 4–5 μg of the chimeric genomic transcripts was applied to single *N. benthamiana* or *Brassica pekinensis* (Chinese cabbage) leaves. All plants were held at 21 °C in a 16 h light/8 h dark daily cycle.

After amplification of pDuMV-derived infectious RNA *in planta*, the 3′ terminal sequences of the progeny genomes were examined. Total RNA was tailed with either adenosine or cytosine using Poly(A) Tailing Kit (Ambion), reverse transcribed with an oligo(dT) or oligo(dG) primer, and submitted to PCR. The amplicons were cloned into pCR 4.0 and four clones from each tailing reaction were sequenced in both directions.

Detection of viral products

Northern blotting to detect viral RNAs was conducted as described (Cho and Dreher, 2006) using digoxigenin (DIG)-labeled DNA probes and chemiluminescent immunodetection of DIG (Roche Applied Science). To detect DuMV and DuMV/3′TY RNA, a probe spanning the DuMV CP ORF (nt 5323–5974) was amplified by PCR using primers NBF (5′ GATCCTCGGTTTCGTCACTTGAGTC) and NBR (5′ GTAATTT-GTTTTGCTGACA). TYMV RNA was detected using a probe corresponding to the CP ORF (nt 5641–6231) (Cho and Dreher, 2006).

Reverse transcription PCR was used for high sensitivity detection of viral RNA. Total RNA extracted as described (Tzanetakis et al., 2007) was used as template. DuMV RNA was amplified using primers DuMVdetF (5′ GAACGACTACACCTCC) (nt 4558–4573) and DuMVdetR (5′ CATCATAAGTGCCTGG) (nt 4729–4745) that amplify a 188 bp fragment of the genome. Primers TYMV 5324F (5′ CACCTCCTTGGC-GAATCACTATG) and DuMV 3′R BstBI/HindIII and primers DuMV 5602F (5′ CATCACTCCTACTCAGCTTGCCATAGAC) and TYMV-DuMV 3′ fusion R were used to detect TYMV/3′Du and DuMV/3′TY RNA, respectively. For DuMV and DuMV/3′TY RNA detection, the PCR program consisted of a denaturation step of 3 min at 94 °C followed by 40 cycles of 30 s each at 94 °C, 58 °C and 72 °C. The same program except for annealing temperature of 60 °C and extension for 2 min was used for TYMV/3′Du amplification. The reactions were terminated with a 10 min extension at 72 °C.

Virus purification and electron microscopy

Virus amplified from wild type or infectious clone-derived RNA in *N. benthamiana* was purified by the method of Lane (1986). For electron microscopy analysis, leaf dips of DuMV-infected *N. benthamiana* or purified virus were loaded on carbon coated grids. The virions were stained with 2% uranyl acetate or 2% ammonium molybdate and were visualized on a CM-12 Philips transmission electron microscope.

Acknowledgments

This work was supported by NSF grant MCB-0235563 awarded to T. W.D. and by the Oregon State University College of Agricultural Sciences and by start-up funds provided by the Arkansas Agricultural Experiment Station to I.E.T. We would like to thank Joshua Powell for electron microscopy.

References

Ahlquist, P., Luckow, V., Kaesberg, P., 1981. Complete nucleotide sequence of brome mosaic virus RNA3. J. Mol. Biol. 153, 23–38.
Bink, H.H., Schirawski, J., Haenni, A.L., Pleij, C.W., 2003. The 5′-proximal hairpin of turnip yellow mosaic virus RNA: its role in translation and encapsidation. J. Virol. 77, 7452–7458.
Bozarth, C.S., Weiland, J.J., Dreher, T.W., 1992. Expression of ORF-69 of turnip yellow mosaic virus is necessary for viral spread in plants. Virology 187, 124–130.
Bransom, K.L., Dreher, T.W., 1994. Identification of the essential cysteine and histidine residues of the turnip yellow mosaic virus protease. Virology 198, 148–154.
Bransom, K.L., Wallace, S.E., Dreher, T.W., 1996. Identification of the cleavage site recognized by the turnip yellow mosaic virus protease. Virology 217, 404–406.
Candresse, T., Morch, M.D., Dunez, J., 1990. Multiple alignment and hierarchical clustering of conserved amino acid sequences in the replication-associated proteins of plant RNA viruses. Res. Virol. 141, 315–329.
Chen, J., Li, W.X., Xie, D., Peng, J.R., Ding, S.W., 2004. Viral virulence protein suppresses RNA silencing-mediated defense but upregulates the role of microrna in host gene expression. Plant Cell 16, 1302–1313.

Cho, T.J., Dreher, T.W., 2006. Encapsidation of genomic but not subgenomic Turnip yellow mosaic virus RNA by coat protein provided in trans. Virology 356, 126–135.
Deiman, B.A.L.M., Koenen, A.K., Verlaan, P.W.G., Pleij, C.W.A., 1998. Minimal template requirements for initiation of minus-strand synthesis in vitro by the RNA-dependent RNA polymerase of turnip yellow mosaic virus. J. Virol. 72, 3965–3972.
Ding, S.W., Howe, J., Keese, P., Mackenzie, A., Meek, D., Osorio-Keese, M., Skotnicki, M., Srifah, P., Torronen, M., Gibbs, A., 1990a. The tymobox, a sequence shared by most tymoviruses: its use in molecular studies of tymoviruses. Nucleic Acids Res. 18, 1181–1187.
Ding, S.W., Howe, J., Mackenzie, A., Skotnicki, M., Gibbs, A., 1990b. Nucleotide sequence of the virion protein gene of belladonna mottle tymovirus. Nucl. Acids Res. 18, 6138.
Dreher, T.W., 1999. Functions of the 3′-untranslated regions of positive strand RNA viral genomes. Annu. Rev. Phytopathol. 37, 151–174.
Dreher, T.W., 2009. Role of tRNA-like structures in controlling plant virus replication. Virus Res. 139, 217–229.
Dreher, T.W., Goodwin, J.B., 1998. Transfer RNA mimicry among tymoviral genomic RNAs ranges from highly efficient to vestigial. NucleicAcids Res. 26, 4356–4364.
Dreher, T.W., Rao, A.L.N., Hall, T.C., 1989. Replication in vivo of mutant brome mosaic virus RNAs defective in aminoacylation. J. Mol. Biol. 206, 425–438.
Dreher, T.W., Tsai, C.H., Florentz, C., Giege, R., 1992. Specific valylation of turnip yellow mosaic virus RNA by wheat germ valyl-tRNA synthetase determined by three anticodon loop nucleotides. Biochemistry 31, 9183–9189.
Dreher, T.W., Tsai, C.H., Skuzeski, J.M., 1996. Aminoacylation identity switch of turnip yellow mosaic virus RNA from valine to methionine results in an infectious virus. Proc. Natl. Acad. Sci. U. S. A. 93, 12212–12216.
Filomatori, C.V., Lodeiro, M.F., Alvarez, D.E., Samsa, M.M., Pietrasanta, L., Gamarnik, A.V., 2006. A 5′ RNA element promotes dengue virus RNA synthesis on a circular genome. Genes Dev. 20, 2238–2249.
Gibbs, A.J., Hecht-Poinar, E., Woods, R.D., McKee, R.K., 1966. Some properties of three related viruses: Andean potato latent, dulcamara mottle, and Ononis yellow mosaic. J. Gen. Microbiol. 44, 177–193.
Goodwin, J.B., Dreher, T.W., 1998. Transfer RNA mimicry in a new group of positive-strand RNA plant viruses, the furoviruses: differential aminoacylation between the RNA components of one genome. Virology 246, 170–178.
Goodwin, J.B., Skuzeski, J.M., Dreher, T.W., 1997. Characterization of chimeric turnip yellow mosaic virus genomes that are infectious in the absence of aminoacylation. Virology 230, 113–124.
Guo, L., Allen, E.M., Miller, W.A., 2001. Base-pairing between untranslated regions facilitates translation of uncapped, nonpolyadenylated viral RNA. Mol. Cell 7, 1103–1109.
Haenni, A.L., Dreher, T.W., 2008. Tymoviruses, Third Ed. Encyclopedia of Virology, Vol. 5, pp. 199–207.
Hellendoorn, K., Michiels, P.J., Buitenhuis, R., Pleij, C.W., 1996. Protonatable hairpins are conserved in the 5′-untranslated region of tymovirus RNAs. Nucleic Acids Res. 24, 4910–4917.
Hellendoorn, K., Verlaan, P.W., Pleij, C.W., 1997. A functional role for the conserved protonatable hairpins in the 5′ untranslated region of turnip yellow mosaic virus RNA. J. Virol. 71, 8774–8779.
Hu, B., Pillai-Nair, N., Hemenway, C., 2007. Long-distance RNA-RNA interactions between terminal elements and the same subset of internal elements on the potato virus X genome mediate minus- and plus-strand RNA synthesis. RNA 13, 267–280.
Jakubiec, A., Drugeon, G., Camborde, L., Jupin, I., 2007. Proteolytic processing of turnip yellow mosaic virus replication proteins and functional impact on infectivity. J. Virol. 81, 11402–11412.
Kadaré, G., Rozanov, M., Haenni, A.L., 1995. Expression of the turnip yellow mosaic virus proteinase in *Escherichia coli* and determination of the cleavage site within the 206 kDa protein. J. Gen. Virol. 76, 2853–2857.
Khan, A.H., Morita, K., del Carmen Parquet, M., Hasebe, F., Mathenge, E.G., Igarashi, A., 2002. Complete nucleotide sequence of chikungunya virus and evidence for an internal polyadenylation site. J. Gen. Virol. 83, 3075–3084.
Koenig, R., Barends, S., Gultyaev, A.P., Lesemann, D.E., Vetten, H.J., Loss, S., Pleij, C.W., 2005a. Nemesia ring necrosis virus: a new tymovirus with a genomic RNA having a histidylatable tobamovirus-like 3′ end. J. Gen. Virol. 86, 1827–1833.
Koenig, R., Pleij, C.W., Lesemann, D.E., Loss, S., Vetten, H.J., 2005b. Molecular characterization of isolates of anagyris vein yellowing virus, plantago mottle virus and scrophularia mottle virus — comparison of various approaches for tymovirus classification. Arch. Virol. 150, 2325–2338.
Koonin, E.V., 1991. The phylogeny of RNA-dependent RNA polymerases of positive-strand RNA viruses. J. Gen. Virol. 72, 2197–2206.
Kozlov, Y.V., Rupasov, V.V., Adyshev, D.M., Belgelarskaya, S.N., Agranovsky, A.A., Mankin, A.S., Morozov, S., Dolja, V.V., Atabekov, J.G., 1984. Nucleotide sequence of the 3′-terminal tRNA-like structure in barley stripe mosaic virus genome. Nucleic Acids Res. 12, 4001–4009.
Lane, L., 1986. Propagation and purification of RNA plant viruses. Methods Enzymol. 118, 687–696.
Mans, R.M., Van Steeg, M.H., Verlaan, P.W., Pleij, C.W., Bosch, L., 1992. Mutational analysis of the pseudoknot in the tRNA-like structure of turnip yellow mosaic virus RNA. Aminoacylation efficiency and RNA pseudoknot stability. J. Mol. Biol. 223, 221–232.
Marchler-Bauer, A., Anderson, J.B., Derbyshire, M.K., DeWeese-Scott, C., Gonzales, N.R., Gwadz, M., Hao, L., He, S., Hurwitz, D.I., Jackson, J.D., Ke, Z., Krylov, D., Lanczycki, C.J., Liebert, C.A., Liu, C., Lu, F., Lu, S., Marchler, G.H., Mullokandov, M., Song, J.S., Thanki, N., Yamashita, R.A., Yin, J.J., Zhang, D., Bryant, S.H., 2007. CDD: a conserved domain database for interactive domain family analysis. Nucleic Acids Res. 35, D237–D240.
Matsuda, D., Bauer, L., Tinnesand, K., Dreher, T.W., 2004. Expression of the two nested overlapping reading frames of turnip yellow mosaic virus RNA is enhanced by a 5′ cap and by 5′ and 3′ viral sequences. J. Virol. 78, 9325–9335.
Matsuda, D., Dreher, T.W., 2004. The tRNA-like structure of Turnip yellow mosaic virus RNA is a 3′-translational enhancer. Virology 321, 36–46.
Matsuda, D., Dreher, T.W., 2006. Close spacing of AUG initiation codons confers dicistronic character on a eukaryotic mRNA. RNA 12, 1338–1349.
Matsuda, D., Dreher, T.W., 2007. Cap- and initiator tRNA-dependent initiation of TYMV polyprotein synthesis by ribosomes: evaluation of the Trojan horse model for TYMV RNA translation. RNA 13, 129–137.
Rozanov, M.N., Koonin, E.V., Gorbalenya, A.E., 1992. Conservation of the putative methyltransferase domain: a hallmark of the 'Sindbis-like' supergroup of positive-strand RNA viruses. J. Gen. Virol. 73, 2129–2134.
Rozanov, M.N., Drugeon, G., Haenni, A.L., 1995. Papain-like proteinase of turnip yellow mosaic virus: a prototype of a new viral proteinase group. Arch. Virol. 140, 273–288.
Segwagwe, A.T., Putnam, M.L., Druffel, K.L., Pappu, H.R., Eastwell, K.C., 2008. Molecular characterization of a new tymovirus from Diascia ornamental plants. Arch. Virol. 153, 1495–1503.
Shin, H.I., Tzanetakis, I.E., Dreher, T.W., Cho, T.J., 2009. The 5′-UTR of Turnip yellow mosaic virus does not include a critical encapsidation signal. Virology 387, 427–435.
Singh, R.N., Dreher, T.W., 1998. Specific site selection in RNA resulting from a combination of nonspecific secondary structure and –CCR– boxes: initiation of minus strand synthesis by turnip yellow mosaic virus RNA-dependent RNA polymerase. RNA 4, 1083–1095.
Skuzeski, J.M., Bozarth, C.S., Dreher, T.W., 1996. The turnip yellow mosaic virus tRNA-like structure cannot be replaced by generic tRNA-like elements or by heterologous 3′ untranslated regions known to enhance mRNA expression and stability. J. Virol. 70, 2107–2115.
Srifah, P., Keese, P., Weiller, G., Gibbs, A., 1992. Comparisons of the genomic sequences of erysimum latent virus and other tymoviruses: a search for the molecular basis of their host specificities. J. Gen. Virol. 73, 1437–1447.
Srinivasan, K.G., Min, B.E., Ryu, K.H., Adkins, S., Wong, S.M., 2005. Determination of complete nucleotide sequence of Hibiscus latent Singapore virus: evidence for the presence of an internal poly(A) tract. Arch. Virol. 150, 153–166.
Stephan, D., Siddiqua, M., Ta Hoang, A., Engelmann, J., Winter, S., Maiss, E., 2008. Complete nucleotide sequence and experimental host range of Okra mosaic virus. Virus Genes 36, 231–240.
Tsai, C.H., Dreher, T.W., 1991. Turnip yellow mosaic virus RNAs with anticodon loop substitutions that result in decreased valylation fail to replicate efficiently. J. Virol. 65, 3060–3067.
Tzanetakis, I.E., Martin, R.R., 2004. Complete nucleotide sequence of a strawberry isolate of Beet pseudoyellows virus. Virus Genes 28, 239–246.
Tzanetakis, I.E., Keller, K.E., Martin, R.R., 2005. The use of reverse transcriptase for efficient first- and second-strand cDNA synthesis from single- and double-stranded RNA templates. J. Virol. Methods 124, 73–77.
Tzanetakis, I.E., Halgren, A., Mosier, N., Martin, R.R., 2007. Identification and characterization of Raspberry mottle virus, a novel member of the *Closteroviridae*. Virus Res. 127, 26–33.
van Dijk, A.A., Makeyev, E.V., Bamford, D.H., 2004. Initiation of viral RNA-dependent RNA polymerization. J. Gen. Virol. 85, 1077–1093.
Weiland, J.J., Dreher, T.W., 1989. Infectious TYMV RNA from cloned cDNA: effects in vitro and in vivo of point substitutions in the initiation codons of two extensively overlapping ORFs. Nucleic Acids Res. 17, 4675–4687.
Wu, B., Pogany, J., Na, H., Nicholson, B.L., Nagy, P.D., White, K.A., 2009. A discontinuous RNA platform mediates RNA virus replication: building an integrated model for RNA-based regulation of viral processes. PLoS Pathog. 5, e1000323.
Yoshikawa, N., Converse, R.H., 1990. Strawberry pallidosis disease: distinctive dsRNA species associated with latent infections in indicators and in diseased strawberry cultivars. Phytopathology 80, 543–548.
Yoshinari, S., Nagy, P.D., Simon, A.E., Dreher, T.W., 2000. CCA initiation boxes without unique promoter elements support in vitro transcription by three viral RNA-dependent RNA polymerases. RNA 6, 698–707.
Zuker, M., 2003. Mfold web server for nucleic acid folding and hybridization prediction. Nucleic Acids Res. 31, 3406–3415.